JOURNAL OF SOLID STATE CHEMISTRY 73, 418–426 (1988)

New Intergrowth Phases in the ZnO–In_2O_3 System

P. J. CANNARD AND R. J. D. TILLEY

Institute of Materials, University College, Newport Road, Cardiff CF2 1TA, Great Britain

Received May 28, 1987; in revised form August 25, 1987

Reaction of ZnO with In_2O_3 at 1100°C produced a series of compounds with layer structures which have been characterized using powder X-ray diffraction and high-resolution electron microscopy. The structures of the phases consist of slabs of wurtzite-type ZnO separated by thin lamellae of In_2O_3, two metal–oxygen layers thick. The distance between the In_2O_3 layers increases with decreasing concentration of In_2O_3. At high In_2O_3 concentrations a homologous series of ordered phases form with compositions given by the series formula $Zn_nIn_2O_{n+3}$, n taking values between 4 and 11 at 1100°C. The In_2O_3 lamellae are disordered at lower concentrations of In_2O_3 and an operationally nonstoichiometric phase is formed.

Introduction

ZnO is widely used as a ceramic varistor, as a catalyst, and in numerous other electronic and chemical applications. In order to enhance its properties for these purposes it is frequently "doped" with other compounds, usually oxides. There has been, to date, very little work on the crystal chemistry of such materials, although the defect structures of these phases are of significant interest. To attempt to partly fill the gap we have investigated a number of systems, including that reported here, ZnO–In_2O_3.

The only previous paper of note that we have found in the literature is by Kasper (*1*). He found that when zinc oxide and indium oxide were reacted, a series of complex structures were produced, as summarized in Table 1. In these phases the two parent compounds were believed to intergrow to form a laminated structure so that slabs of ZnO, cut perpendicular to the hexagonal c-axis, were bounded at regular intervals by an interposing slab of indium oxide, as shown schematically in Fig. 1. This resulted in materials which had hexagonal or rhombohedral symmetry and long c-axes. Because of the complexity of these compounds, the early studies did not answer all the structural questions associated with these phases, and so the present investigation was initiated. As X-ray diffraction is not well suited to the characterization of such long unit cell materials, and more particularly of any disordered phases which are likely to occur, we have concentrated on electron microscope analysis in this study. A number of new phases have been found and the nature of disordered ZnO crystals when only small quantities of In_2O_3 are present has been clarified. We report the preliminary results of the study in this paper.

0022-4596/88 $3.00

TABLE I

PHASES IN THE $ZnO-In_2O_3$ SYSTEM (*1*)

Composition	a_0 (nm)	c_0 (nm)
$Zn_2In_2O_5$	0.3376 ± 0.0001	2.3154 ± 0.001
$Zn_3In_2O_6$	0.3355 ± 0.0001	4.2515 ± 0.002
$Zn_4In_2O_7$	0.3339 ± 0.0002	3.3520 ± 0.002
$Zn_5In_2O_8$	0.3327 ± 0.0001	5.8114 ± 0.002
$Zn_7In_2O_{10}$	0.3313 ± 0.0001	7.3620 ± 0.004

TABLE II

PREPARATIONS MADE AT 1100°C

$ZnO:In_2O_3$	Time (days)
1:1	3
1:1	7
5:1	3
5:1	7
10:1	3
10:1	7
20:1	7
35:1	7
50:1	7

Experimental

Johnson Matthey "specpure"-grade zinc oxide and indium oxide were used in all preparations. Appropriate quantities of each compound were weighed and well mixed in an agate mortar before being pressed into 1-cm-diameter pellets. These were placed on a sheet of platinum and heated in air, the temperature being monitored using a platinum/platinum 13% rhodium thermocouple. After heat treatment the pellets were slowly cooled in air. Table 2 lists compositions and thermal history of the samples prepared.

After reaction a part of each sample was examined by powder X-ray diffraction using a Hägg–Guinier focusing camera employing strictly monochromatic $CuK\alpha_1$ radiation and KCl (a_0 = 0.62923 nm at 25°C) as an internal standard. Selected samples, listed in Table 3, were also examined by transmission electron microscopy. Samples for electron microscopy were prepared by crushing a small amount of the compound to be studied under *n*-butanol in an agate mortar. A drop of the resulting suspension was placed on a copper grid previously cov-

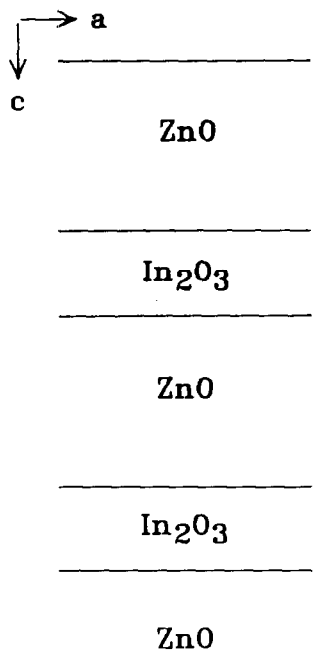

FIG. 1. Schematic arrangement of ZnO and In_2O_3 layers along the *c*-axis.

TABLE III

ELECTRON MICROSCOPE PHASE ANALYSIS

	Composition, $ZnO:In_2O_3$[a]						
Phase	1:1[a]	1:1	5:1[a]	10:1	20:1	35:1	50:1
$Zn_4In_2O_7$	3	—	—	—	—	—	—
$Zn_5In_2O_8$	2	3	4	1	1	—	—
$Zn_6In_2O_9$	—	—	1	—	—	—	—
$Zn_7In_2O_{10}$	—	1	5	7	1	2	1
$Zn_9In_2O_{12}$	—	—	—	3	3	2	—
$Zn_{11}In_2O_{14}$	—	—	1	—	1	1	—
Disordered	—	—	—	3	2	—	1
Total	5	4	11	14	8	5	2

[a] All samples heated for 7 days except these which were heated for 3 days.

ered with a holey carbon film. Crystals were examined in a JEM 200CX transmission electron microscope fitted with a high-resolution top entry goniometer stage and operated at 200 kV with a LaB_6 filament. The objective lens had a C_s of 1.2 mm and an objective aperture was not used. For these preliminary studies electron microscope images were obtained by using the (001) row of systematic reflections. The resulting images were mostly photographed at a magnification of 500,000×.

Results

Powder X-ray Diffraction

The X-ray films revealed the presence of residues of the starting materials in each preparation, as well as other phases. The powder pattern from the 50 ZnO : 1 In_2O_3 sample showed the presence of ZnO reflections with slightly broadened (101) and (102) lines, a trace of In_2O_3, and some diffuse lines indicating the presence of one or more ZnO : In_2O_3 ternary phases. The 35 ZnO : 1 In_2O_3 sample was similar to the 50 ZnO : 1 In_2O_3 sample, but showed more new lines, and the remaining ZnO lines were slightly broader. The 20 ZnO : 1 In_2O_3 film showed a greater concentration of the ternary phases, with some of the lines from these materials being broad while others were sharp. In the 10 ZnO : 1 In_2O_3 sample the ZnO lines were fairly broad and were slightly displaced from those in the other films, and in the 5 ZnO : 1 In_2O_3 preparation, these lines were difficult to distinguish from those belonging to the ZnO : In_2O_3 phases. Finally in the 1 ZnO : 1 In_2O_3 film the ZnO lines had virtually disappeared but the In_2O_3 lines were still present and sharp. All the remaining lines belonged to the ZnO : In_2O_3 phases. There was little or no difference between the samples reacted for 3 days and for 7 days.

None of the films were measured because the preparations were clearly not at equilibrium. Despite this drawback, the films revealed that the ZnO lines broadened on reaction with In_2O_3, while the In_2O_3 lines always remained sharp, indicating that the ZnO was capable of a nonstoichiometric phase range while In_2O_3 remained stoichiometric within the precision of this technique.

Electron Diffraction Patterns

The diffraction patterns bear a strong resemblance to the diffraction pattern expected from ZnO. The direction of greatest interest is c^*, here characterized by strong ZnO (002) reflections. In addition to the ZnO reflections, superlattice reflections and streaking, in variable amounts depending upon the degree of order present in the sample, were also usually present. Figure 2 shows typical examples. The number of superlattice reflections observed in the samples allows the phase composition to be designated, as discussed below. The phases identified in this way are listed in Table 3.

Electron Microscopy

The images, typical examples of which are shown in Fig. 3, reveal that the structures of the phases are made up of slabs of ZnO interleaved with faults. The spacing between the faults decreased as the overall amount of In_2O_3 in the preparation increased suggesting that the faults are lamellae of In_2O_3. The faults can be well ordered, as in Fig. 3a, from a sample of composition 5 ZnO : 1 In_2O_3, to very disordered, as illustrated in Fig. 3b, from a sample of composition 20 ZnO : 1 In_2O_3. There was no evidence of a phase boundary in the ZnO-rich preparations. Instead the faults became further apart and more random in position as the ZnO composition was approached.

At the thin edges of the crystal, the (002) lattice fringes of ZnO, with a spacing of 0.2605 nm, were clearly visible between the faults. If the faults are made up of thin slabs of In_2O_3 this should result in sufficient dif-

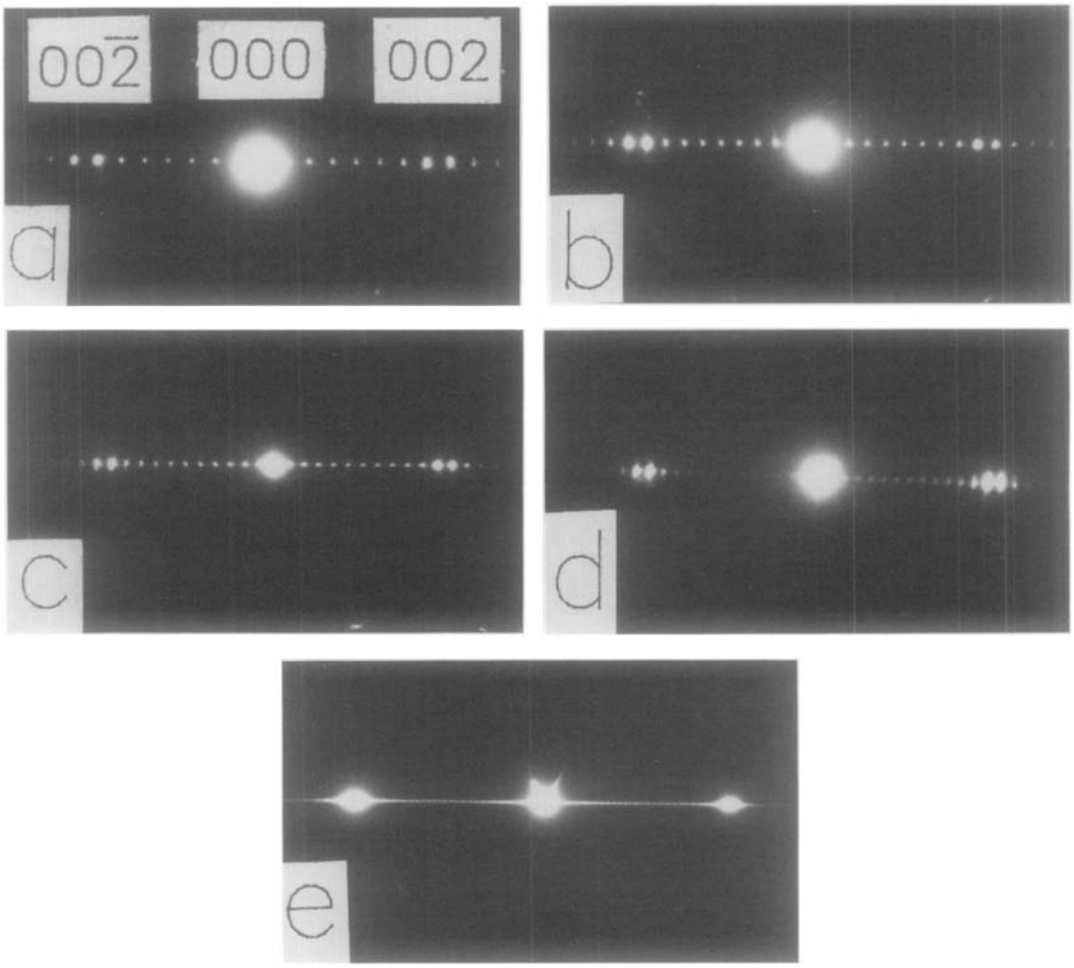

FIG. 2. Electron diffraction patterns of (a) $Zn_5In_2O_8$ (b) $Zn_7In_2O_{10}$ (c) $Zn_9In_2O_{12}$ (d) $Zn_{11}In_2O_{14}$ (e) disordered $Zn_nIn_2O_{n+3}$ containing respectively 8, 10, 12, 14, and ∞ number of spots from (000) to the second intense spot. An infinite number of spots results in continuous streaking along the c^*-axis.

ference in potential to allow the two types of layer to be distinguished in terms of contrast. This was not found to be easy in practice, and the number of layers in a fault had to be determined by measurement. For this, focal series of micrographs were selected, and from these, micrographs which were underfocus by about 60 nm were examined. Computer simulations indicated that in this case the dark fringes visible on micrographs corresponded to metal atom planes in the ZnO parts of the materials and so provided an internal scale. Measurements of the micrographs using an optical densitometer indicated that there were two different types of dark fringes in the faults separated from the neighboring ZnO slabs by three wider white fringes. This is consistent with the interpretation of the fault structure as consisting of a slice of In_2O_3 structure two {111} planes in thickness and confirms a contrast difference between the ZnO and In_2O_3 layers. Figure 4 shows a typical micrograph and microdensitometer trace.

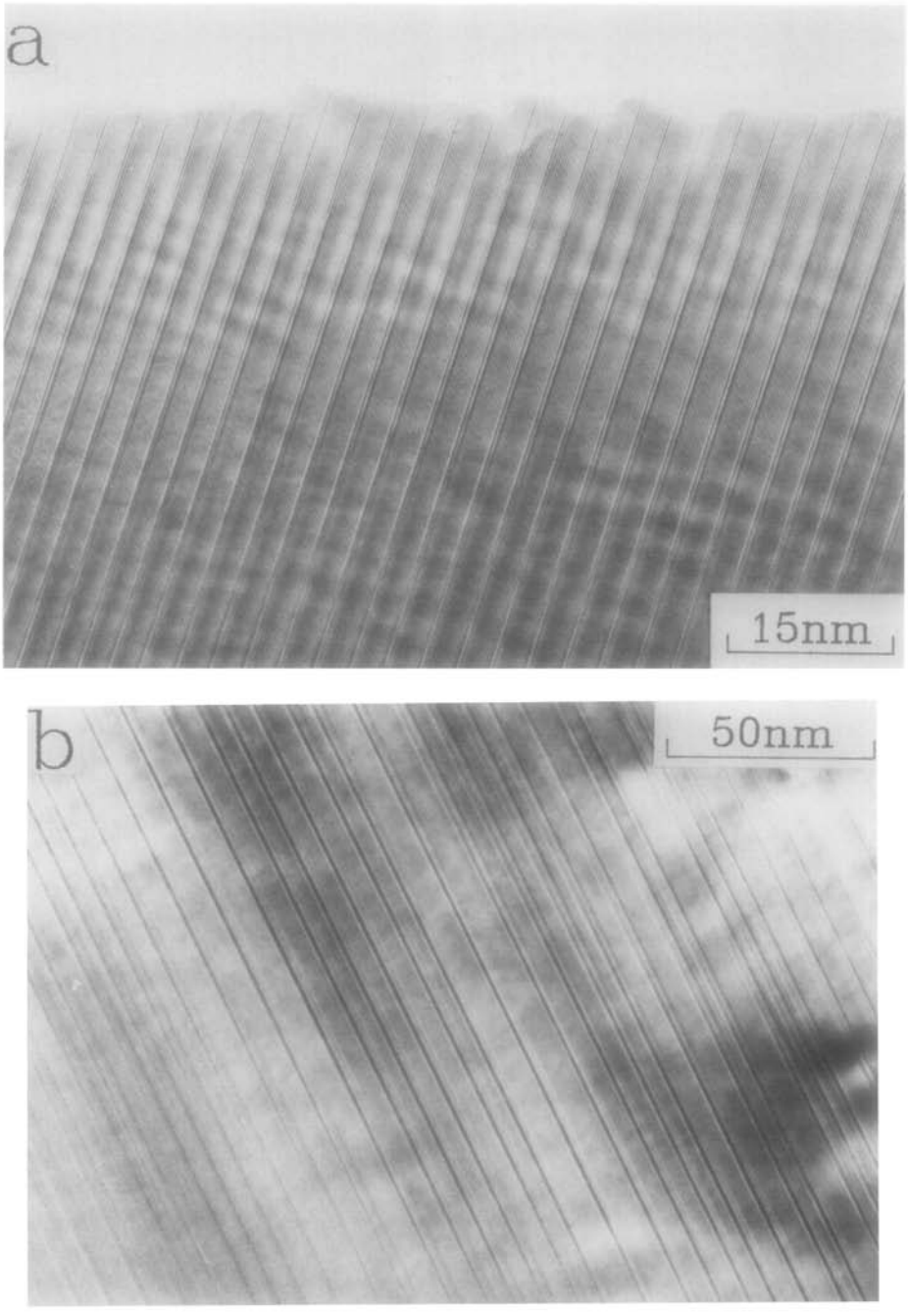

FIG. 3. (a) (001) Lattice fringes in a well-ordered crystal of $Zn_{10}In_2O_{13}$. The closely spaced fringes represent (002) ZnO lattice planes and the heavier dark fringes represent the In_2O_3 intergrowths. (b) A crystal of $Zn_nIn_2O_{n+3}$ in which only the In_2O_3 slabs are imaged, revealing considerable disorder.

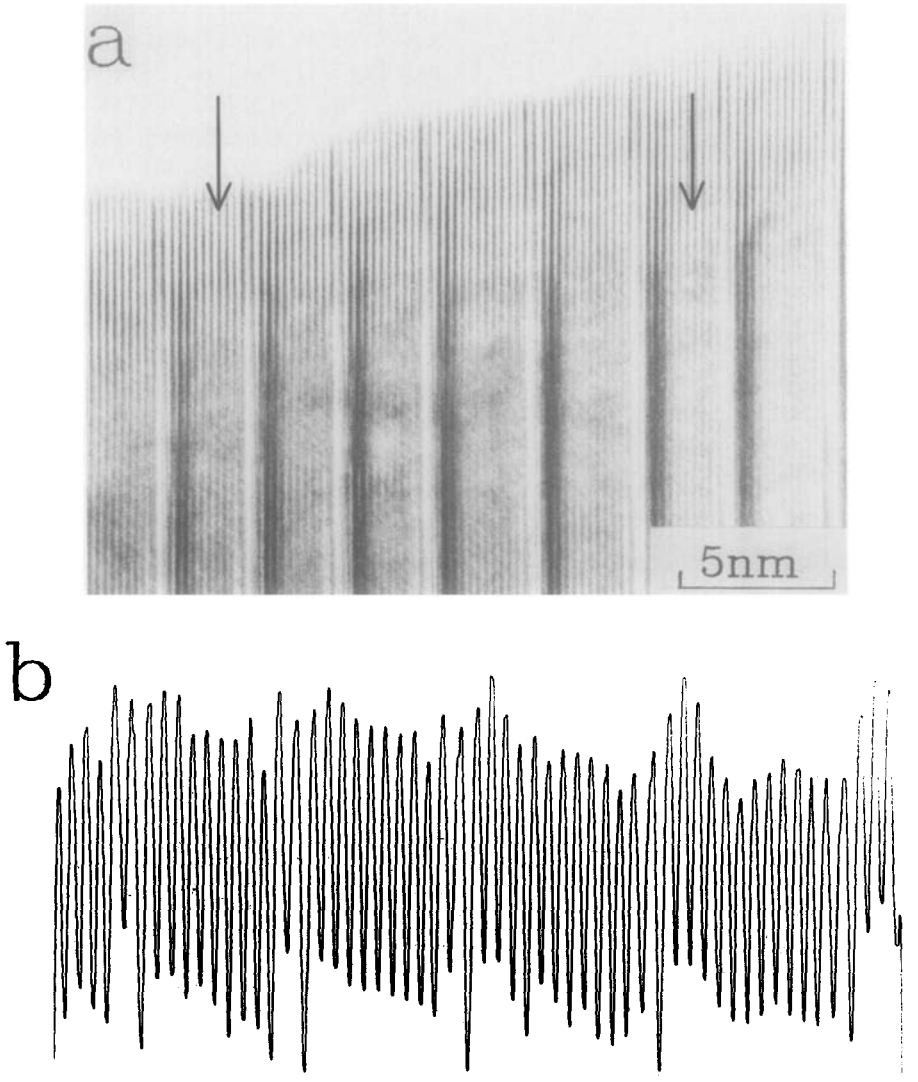

FIG. 4. (a) Micrograph of $Zn_9In_2O_{12}$ crystal showing (001) lattice fringes. (b) Microdensitometer trace across (a) between the two arrows.

Discussion

The results show that the structures formed by reaction of ZnO and In_2O_3 are comprised of slabs of ZnO separated by faults. The faults consist of slices of the In_2O_3 structure two {111} planes in thickness. At the ZnO-rich end of the composition range studied these faults are disordered and an operational nonstoichiometric phase range exists. As the In_2O_3 concentration increases the faults become ordered and assimilated into the structure to form a homologous series of new phases. A schematic illustration of this structure is shown in Fig. 5 for $Zn_4In_2O_7$.

In order to consider the nature of the homologous series it is necessary to consider

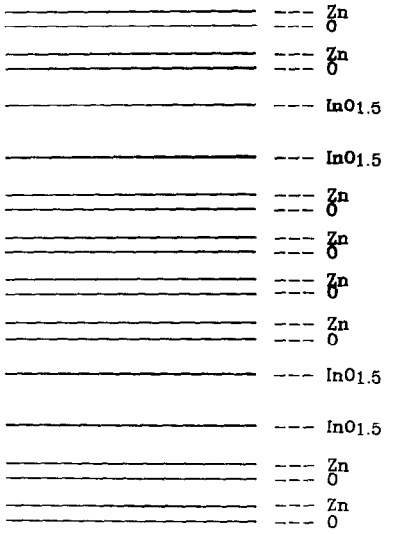

FIG. 5. The stacking of Zn, O, and $InO_{1.5}$ layers perpendicular to the c-axis of the $Zn_nIn_2O_{n+3}$ phases. The specific example is of $Zn_4In_2O_7$. Other members of the series differ only in the number of Zn and O layers present.

the crystallographic aspects of the two parent compounds. ZnO has the wurtzite structure, with $a_0 = 0.325$ nm, $c_0 = 0.521$ nm (*2*), and In_2O_3 the cubic bixbyite structure, with $a_0 = 1.0117$ nm (*3*). This structure is closely related to the fluorite structure-type and the In atoms in In_2O_3 are in a face centered cubic array, as are the metal atoms in the fluorite structure. The two structures intergrow along the hexagonal c-axis direction. It is reasonable to assume that the cubic phase will thus intergrow as slabs of {111} orientation in accord with the measurements of the fault plane spacings and the model illustrated in Fig. 5.

In the ZnO structure, the metal and oxygen atoms are separated; each atom type occupying alternate {001} planes. In the In_2O_3 structure, each {111} plane contains both oxygen and indium atoms. This allows us to calculate both the formulas of the ordered phases and the unit cell dimensions. To illustrate this, suppose that we have an ordered phase made up of blocks of ZnO structure n Zn and n O planes in thickness, separated by single faults each consisting of two In_2O_3 {111} planes. The total composition of the ZnO slabs will be nZnO, as the composition of each layer per wurtzite unit cell is either $1 \times$ Zn or $1 \times$ O. The composition of each layer in the {111} sequence of In_2O_3 is the same as the composition of the oxide, In_2O_3. In the hexagonal wurtzite size unit cell of the intergrowth phases, though, each layer only has one metal atom per unit cell, giving each layer a composition of $InO_{1.5}$. Each fault will thus add a composition of In_2O_3 per $(ZnO)_n$ slab to the formula. Each member of the series will thus have a composition of $In_2Zn_nO_{n+3}$. A similar formula was derived by Kasper (*1*) from composition data. The formulas of the phases included in Table 4 are derived from this formula.

The idealized unit cells of the phases can be calculated from this model quite simply. The a parameter of the hexagonal cell will be about equal to that of ZnO, i.e., 0.325 nm. The c parameter repeat will be composed of a contribution from the In_2O_3 fault layer and the correct number of ZnO layers. In the interior of the ZnO slabs each layer will be separated by the ZnO (002) spacing of 0.2605 nm. In the phase Zn_nIn_2

TABLE IV

IDEALIZED LATTICE PARAMETERS

Phase	Calculated c (nm)	c_{red} (*1*)	δ^a
$Zn_{12}In_2O_{15}$	3.74	—	—
$Zn_{11}In_2O_{14}$	3.48	—	—
$Zn_{10}In_2O_{13}$	3.22	—	—
$Zn_9In_2O_{12}$	2.96	—	—
$Zn_8In_2O_{11}$	2.70	—	—
$Zn_7In_2O_{10}$	2.44	2.4540	−0.0140
$Zn_6In_2O_9$	2.18	—	—
$Zn_5In_2O_8$	1.92	1.9371	−0.0171
$Zn_4In_2O_7$	1.66	1.6760	−0.0160
$Zn_3In_2O_6$	1.40	1.4172	−0.0172
$Zn_2In_2O_5$	1.14	1.1577	−0.0177

[a] δ, Difference between c and c_{red}.

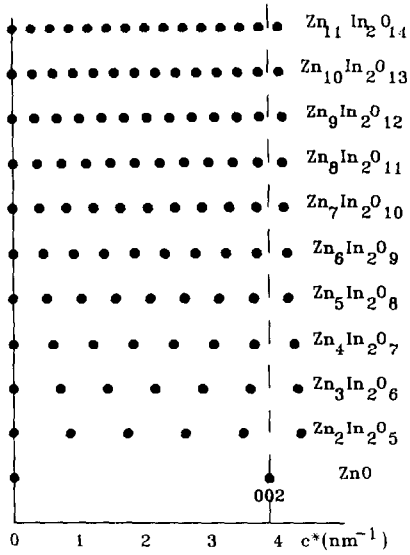

FIG. 6. Schematic illustration of the appearance of the (001) diffraction pattern rows for $Zn_nIn_2O_{n+3}$ phases. The dashed line shows the position of the ZnO (002) reflection, and in the ordered phases the two spots on either side of this line will be of greatest intensity.

O_{n+3} there will be $(n - 1)$ of these layers. Similarly the two $InO_{1.5}$ will be separated by d_{111} In_2O_3, which for a cubic unit cell of 1.0118 nm is equal to 0.292 nm. It is then necessary to estimate the separation of the two $InO_{1.5}$–ZnO per repeat unit. We have assumed that the large In atoms dominate this separation rather than the smaller Zn atoms, and so have assumed that this spacing is also equal to d_{111} In_2O_3. For the phase $Zn_nIn_2O_{n+3}$, the lattice repeat in the c direction will be equal to $[(n - 1) \times 0.2605 + 3 \times 0.292]$ nm. The idealized unit cells quoted in Table 4 are calculated from this formula. From these dimensions it is simple to calculate the disposition of the superlattice spots along the c^* direction on a diffraction pattern. The results are shown in Fig. 6. With this information it is possible to identify the phases in each of the samples prepared without recourse to a measurement of the powder X-ray patterns, which, in the present samples were too disordered to be of value. The formulas in Table 3 were derived from this information.

The previous analysis allows one to determine that the ordered phases found at 1100°C are given by the formula $Zn_nIn_2O_{n+3}$ with n taking all values between 4 and 11. The new phases found are $Zn_6In_2O_9$, $Zn_9In_2O_{12}$, and $Zn_{11}In_2O_{14}$ although neither $Zn_5In_2O_8$ nor $Zn_7In_2O_{10}$ were found by Kasper in preparations at 1100°C. An interesting point appears from a study of Table 3. It is seen that the odd members of the series predominate at 1100°C. This indicates that the stability of the odd members of the series is greater than that of the even members by an appreciable amount. It is possible that this is due to differences in elastic strain energy, as calculations have shown that elastic strain is of importance in stabilizing some members of homologous series over others in both crystallographic shear structures (*4*) and in chemically twinned phases (*5*). In Kasper's study (*1*) two even members of the series are listed, as detailed in Table 1. These, however, were prepared at higher temperatures than in the present experiments, which suggests that the members of the series which are found are rather temperature sensitive. In addition, Kasper reports two other phases, $Zn_2In_2O_5$ and $Zn_3In_2O_6$, which are more In_2O_3-rich than any of the compounds found in this study. This is an indication that the phase range spanned by the homologous series expands as the temperature increases, in a similar way to that reported in the Ga_2O_3–TiO_2 system (*6*).

The present results have confirmed the presence of both an operationally nonstoichiometric phase range in the ZnO–In_2O_3 system and an homologous series of phases containing planar faults. A model has been proposed for the faults which is in accord with the geometrical and crystallographic parameters of the phases found. However, the three-dimensional nature of the faults and the stacking of the metal and oxygen

atom planes across the faults has yet to be determined. In addition, it is still open to some doubt as to whether the same fault structure suggested in this paper persists across the whole of the phase range and at all temperatures. To answer these questions and to clarify the existing temperatures of the various phases discovered further experiments are in progress. These will be reported in due course.

Acknowledgments

P.J.C. is indebted to Sandvik Hard Materials Ltd. and the SERC for financial support during this investigation.

References

1. H. KASPER, *Z. Anorg. Allg. Chem.* **349,** 113 (1967).
2. R. W. G. WYCKOFF, "Crystal Structures," 2nd ed., Vol. 1, p. 111, Interscience, New York (1964).
3. M. MAREZIO, *Acta Crystallogr.* **20,** 723 (1966).
4. E. IGUCHI AND R. J. D. TILLEY, *Philos. Trans. R. Soc. London Ser. A* **286,** 55 (1977).
5. K. AIZAWA, E. IGUCHI, AND R. J. D. TILLEY, *J. Solid State Chem.* **48,** 284 (1983).
6. S. KAMIYA AND R. J. D. TILLEY, *J. Solid State Chem.* **22,** 205 (1977).